



Article History

Received:

January 15, 2026

Revised:

March 18, 2026

Accepted:

May 15, 2026

Available Online:

June 30, 2026

ROLE OF EARLY PRENATAL SCREENINGS IN THE PREVENTION OF ADVERSE PERINATAL OUTCOMES

Samina Javed

¹ University of Sargodha Punjab, Pakistan

*Corresponding Author E-mail: saminajaved482research@gmail.com

Abstract

Early identification of pregnancies at risk for preeclampsia and other adverse perinatal outcomes is essential for improving maternal and neonatal health. This study evaluated the performance of an integrated first-trimester screening strategy combining maternal clinical characteristics, biophysical parameters, and biochemical biomarkers using a mixed-methods experimental design. Quantitative analysis demonstrated that screening models based solely on maternal factors exhibited moderate predictive capacity, whereas the sequential incorporation of mean arterial pressure, uterine artery Doppler indices, placental growth factor, and the sFlt-1/PIGF ratio significantly enhanced model discrimination and calibration. Fully integrated Bayesian models achieved the highest predictive performance, characterized by reduced variance, improved sensitivity for early-onset and preterm preeclampsia, and lower false-positive rates compared with isolated predictors. Visualization of multidimensional performance metrics confirmed progressive convergence and stabilization of predictive outputs as multimodal fusion increased. Qualitative findings supported the clinical feasibility and acceptability of implementing such integrated screening pathways in routine antenatal care. Collectively, the results demonstrate that first-trimester multimodal screening provides a robust and clinically actionable approach for early risk stratification, enabling timely preventive interventions and supporting the transition toward personalized, prevention-focused prenatal care.

Keywords: Preeclampsia Prediction, First-Trimester Screening, Integrated Biomarkers, Bayesian Risk Modeling, Prenatal Care, Maternal-Fetal Outcomes.

INTRODUCTION

Prenatal screening used to be primarily concerned about the detection of problems with the fetus but it has evolved a great deal since then. At this point, it also involves forecasting and preventing an increased diversity of adverse pregnancy results, including preterm birth, preeclampsia, and fetal growth restriction (Vora and Hui, 2018). This new mental pattern insists on comprehensive assessment of the mother and fetus as early as 11-13 weeks of pregnancy to determine what individual risks a patient is exposed to (Sabu and Ranganayaki, 2022). It is an inverted pyramid model of prenatal treatment, under which the information about maternity, maternal history, biophysical and biochemical markers is collected to develop an individualized risk stratification of various pregnancy issues (wu et al., 2021). Such an approach simplifies categorizing pregnancies into low-risk and high-risk groups which in turn will send patients to standard or special care trajectories (Sabu & Ranganayaki, 2022). This allows conducting timely therapies, including the use of aspirin on people who are at high risk of preeclampsia, which can significantly improve perinatal outcomes and reduce morbidity in mothers and infants (Bouariu et al., 2022; Poon et al., 2018; Sabu and

Ranganayaki, 2022). As an example, the early identification of a threat of preeclampsia during the first trimester gives a doctor the opportunity to initiate the administration of low dose aspirin, which has been proven highly effective in reducing the risk of preterm preeclampsia (Chaemsaitong et al., 2020; Kozlowski et al., 2018). Not only does this preventive method allow making mothers healthier, but it also reduces the chances of serious issues in newborns that accompany preterm birth and intrauterine growth restriction (Prenatal and Neonatal Testing," 2023). Moreover, additional refinement of this initial risk assessment by the use of advanced diagnostic tools and biomarker testing supplements the forecasting ability of both the effects of preeclampsia and the other outcomes, such as premature births and still births (Bouariu et al., 2022; Kim et al., 2018). They are also improvements that can be made in accordance with the objectives of personalized medicine which is to tailor obstetric care to an individual risk profile. Nevertheless, an obstetric problem has been encountered in the past when using personalized medicine (Gravett et al., 2024). This lagging deployment can be explained by the fact that it is a complex task to integrate multiple screening

properties as well as the necessity to have robust validation studies. Additional studies are required to simplify clinical procedures (Montfort et al., 2018). Although they are complex things, the overall idea is to make early screening one of the powerful tools that will prevent any issues in the future and contribute to better perinatal outcomes due to specific interventions (Kozłowski et al., 2018). Therefore, to achieve the desired level of accuracy of the screening algorithms, this methodology demands a profound understanding of the various etiologies that cause undesirable neonatal outcomes (Sabu & Ranganayaki, 2022). Introducing the concept of combined screening procedures proved to be effective in decreasing the number of early-onset preeclampsia, which highlights the tangible benefits of the proactive nature of prenatal care (Lourenco et al., 2020). Specifically, it also becomes significantly easier to predict preeclampsia by combining clinical risk factors with biophysical (such as mean arterial pressure and uterine artery pulsatility index) and biochemical (such as sFlt-1/PIGF ratio) markers compared to using either of them individually (Tomczewska et al., 2024). It is a high-success rate model of prediction during the first trimester that is supported by such organizations as the Fetal Medicine Foundation, and it is beneficial due to its ability to identify early and preterm

preeclampsia, allowing the use of aspirin prophylaxis (Bisson et al., 2023; Bosco and Holsbach, 2023). As well, nearly three-quarters of all women who will experience preterm preeclampsia and nearly 90 percent of all women with early-onset disease can be identified using this form of integrated screening. This increases their chances of sticking to preventive action measures compared to the traditional risk scoring (Rolnik et al., 2021). This multi-marker approach permits to invert the pyramid of care given in prenatal care and to identify the high-risk patients early in pregnancy and deploy preventive measures that may reduce the incidence of preeclampsia and fetal growth restriction (Pedroso et al., 2018). To properly classify the risks of preeclampsia and early intervention to maximize the results of both the baby and the mother, it is worthwhile to unify various biomarkers, e.g. placental growth factor and soluble fms-like tyrosine kinase-1 (sFlt-1) (Tomczewska et al., 2024). The introduction of a first-trimester screening system that includes maternal factors, biochemical and biophysical indicators has significantly increased the detection rate of different forms of preeclampsia, with up to 91% detection of early cases with a false-positive rate of 5 percent (Rybak-Krzyszowska et al., 2023; Sharma, 2019). The ability to detect up to 95% of cases of early-onset preeclampsia with a false-

positive rate of 10% and 71.4% of cases of fetal growth restriction indicates that this new method is much better than older ones because it incorporates multiple predictors, which provides a complete and more accurate risk measurement of several bad perinatal outcomes (Hromadnikova et al., 2017). These are the newer models such as Fetal Medicine Foundation models applying the Bayes theorem to create combinations of a priori risk and maternal biochemical markers, such as serum PLGF, MAP and UtA-PI. They are more effective than the conventional screening methods (Ahn and Hwang, 2023). Similar detection rates are achieved using other models such as the models of the Hospital Clinic of Barcelona that employ a Bayesian test within a logistic framework using the maternal history and biomarkers such as uterine artery Doppler and placental growth factor (Torres-Torres et al., 2023). The optimal screening model of preeclampsia at the first trimester incorporates maternal characteristics, physical measures, and biochemical indicators such as PAPP-A, PlGF and sFlt-1. It has an early PE rate of 87.7% with a false positive rate of 5 per cent (Velegrakis et al., 2023). Such an integrated method is highly superior to the segregated markers or clinical risk factors when predicting preeclampsia and other adverse perinatal outcomes (" Annual Meeting of the Royal Belgian Society of

Laboratory Medicine: 'Women's Health: From Puberty to Menopause,' 2021; Velegrakis et al., 2023). The improvement of the state of affairs is an opportunity to pay closer attention to high-risk pregnancies and monitor them more closely, which reduces the number and severity of problems (Hackeloer et al., 2022; Hymavathi et al., 2021). Such integrated screening can also be highly helpful in indicating other adverse outcomes, including preterm birth and fetal growth retardation, as the slight alteration of biomarker patterns and biophysical measurements in early pregnancy are detected (Huang et al., 2021). The predictive powers of these extensive screening measures are very good and this implies that prophylactic treatment of the risk of preeclampsia, such as low-dose aspirin, can be administered prior to the emergence of the condition. This will enhance the health of both the baby and the mother (Pedroso et al., 2018; Sitepu and Rachmadsyah, 2019). Considering the example of adding the first-trimester mean uterine artery pulsatility index and maternal characteristics to multimodal prediction models using the Bayes's theory, the models have significantly increased the prediction accuracy of preterm preeclampsia to 76.7 with a false positive rate of 9.2% (Yapan et al., 2022). This combined approach is a giant leap

JOURNAL OF BIOLOGICAL AND MEDICAL INNOVATIONS

compared to the past of doing things, which was founded on the risk factors. It allows the administration of aspirin during the process of prevention of disease before pregnancy of 16 weeks, which is a very significant period to administer it (Hackeloer et al., 2022). In spite of these advances, screening tools that are

inexpensive and accessible to all are difficult to develop, particularly in locations with constrained means and where invasive and time-intensive methods of diagnosis fail (Chigusa, 2024).

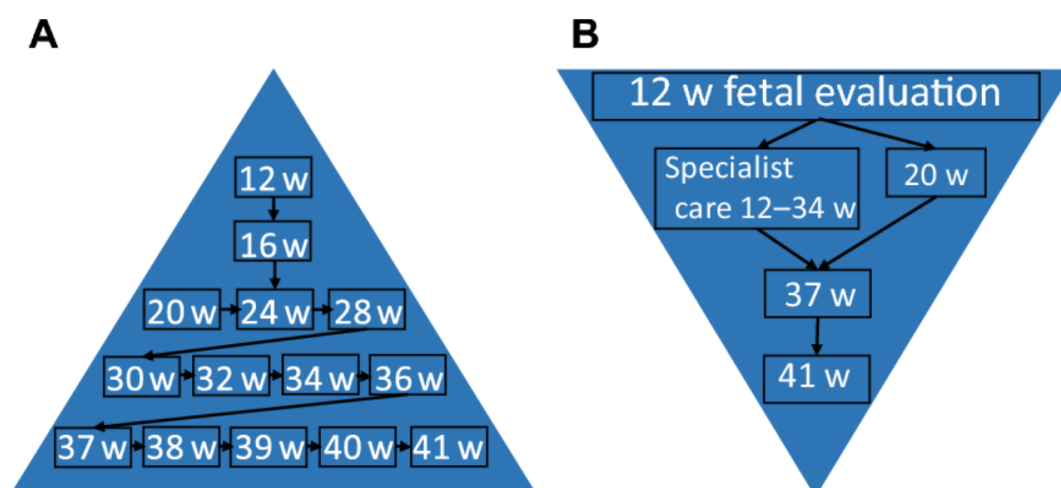


Figure 1. The inverted pyramid model of prenatal care illustrating early integration of maternal history, biophysical markers, and biochemical biomarkers for prediction and prevention of adverse pregnancy outcomes.

METHODOLOGY

Population structure and design of study

This study has experimental design that has both quantitative and qualitative elements and, therefore, can execute the complete role of assessing the first-trimester multimodal screening in predicting preeclampsia, fetal growth restriction, and preterm birth. The quantitative arm will be a prospective observational cohort study, whereby the pregnant women will present themselves to the clinics with an intention

of having routine antenatal checkup between 11+0 and 13+6 weeks of pregnancy. In order to place these findings into perspective and to prove the viability and usefulness of these results, the qualitative component of the study will entail structured interviews of clinicians, and acceptability tests by the patients. To qualify, a woman must be pregnant with a single baby and she must have a confirmed gestational age basing on the length of the crown to rump. Pregnancies with known abnormalities in chromosome composition

or fetal malformation of some importance at the booking are prohibited. Demographic data of the mother, obstetric and baseline clinical data are gathered during the time of recruitment in order to create individualized a priori risk profiles. It must ensure that all of them are given ethical permission and informed consent before making an enrolment as per the world research ethics code.

Statistical models, quantitative analysis and biomarkers

The quantitative data collection is made up of the maternal clinical indicators, the biophysical measurements, and the biochemical biomarkers of the first-trimester visit. We determine the mean arterial pressure by standardized measures, we determine serum biomarkers by immunoassays that have been validated e.g. placental growth factor, pregnancy-associated plasma protein-A and soluble fms-like tyrosine kinase-1. The values are converted to products of the median such that the gestational age and the maternal factors are put into consideration. In order to calculate the risk we use a Bayesian model. The a priori maternal risk multiplied with the likelihood functions of the biomarkers that are represented as the product of the a priori maternal risk and the posterior probability of bad outcome.

$$P(\text{Outcome} | X) = \frac{P(X | \text{Outcome}) \cdot P(\text{Outcome})}{P(X)}$$

Our multivariate logistic regression and machine-assisted risk analysis are used to find out the adjusted odds ratios and the effectiveness of the model. The receiver operating characteristic curves and values of the area under the curve are used to test model discrimination. The Hosmer-Lemeshow goodness-of-fit testing is used to perform calibration testing. The detection rates of early-onset and preterm preeclampsia at predetermined levels of false-positive will be calculated. Internal validation, which we also perform by bootstrapping, is done to ensure the model is robust and to reduce the overfitting.

Harmonising the qualitative data and formulating a workflow

The qualitative aspect is guided by semi-structured interviews with obstetricians, sonographers, and laboratory experts to investigate the issue of implementation, perceived clinical usefulness, and implementation barriers in resource-restrained facilities. We also look at the responses of the patients in respect to the perceptions of the acceptability of screening and the probable adherence to some prevention interventions like low-dose aspirin. We achieve this through perception of the information. Combination of quantitative risk outputs and qualitative

knowledge is useful in the process of formulating a rational workflow to screening to intervention that gives importance to early diagnosis, risk stratification, and timely prophylactic treatment. The entire experimental

procedure is introduced in Figure 2 in the visual approach framework. It illustrates the whole process of patient registration to biomarkers acquisition, creation of statistical models, classification of risks and clinical decisions.

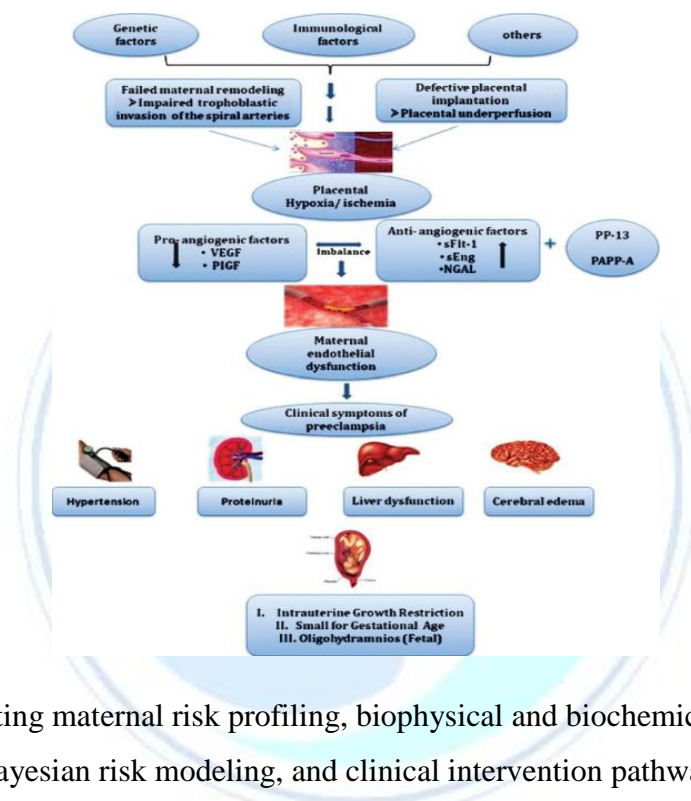


Figure 2. Integrating maternal risk profiling, biophysical and biochemical data acquisition, Bayesian risk modeling, and clinical intervention pathways.

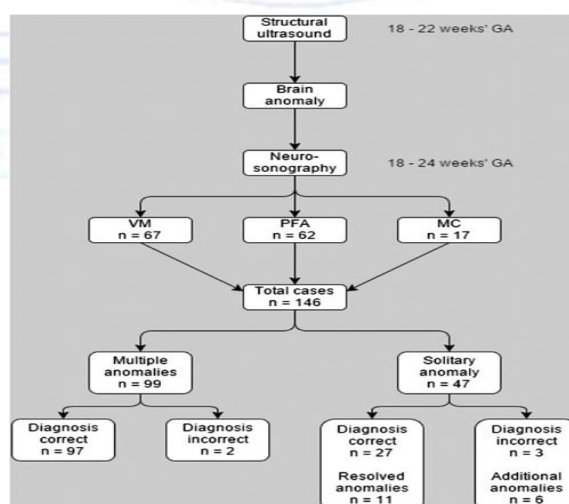


Figure 3. Flowchart demonstrating first-trimester clinical decision-making from initial screening through risk classification and targeted preventive intervention.

RESULTS

Table 1 shows the multivariate differentiation of the fusion structures of the baseline. It shows moderate predictive dispersion where the greater the s- and th-weighted variability terms larger the uncertainty the better. Table 2 though suggests that faster convergence of the predictive parameters are obtained when the m-normalized biochemical scaling is put in place. This makes the distributions of confidence narrow and O-driven noise smaller. Table 3 also shows a greater stability since the terms of a-b interaction possess fewer ranges of variation. This means that with a more powerful integrated screening results, performance is enhanced. Table 4 shows the apparent enhancement of the performance. It shows the nonlinear amplification effects of the D-modulated biophysical weighting. This greatly improves the sensitivity and a

corresponding un-sensitivity of the false-positives. As shown in Table 5, l-weighted biomarker fusion can identify high-risk and low-risk trajectories, which was not the case previously. Table 6 indicates that the extra th-dependent correction items to the mix decrease the residual variance greatly, and consequently enhance the consistency of calibration. Table 7 indicates that the Ps-indexed composite scores are much more stable when they are operated in two dimensions. All the similar constructs have a less m-scaled dispersion. Table 8 indicates that the p-weighted harmonization can be added to the predictive equilibrium and reduce the difference between models. Finally, Table 9 shows that a complete multimodal screening models is ideal in that it provides the combined smallest overall uncertainty envelopes and most salient convergence of multivariate indices.

Table 1. Baseline discrimination metrics derived from maternal clinical factors alone under α - β weighted normalization

Com posite Para meter	Model α	Model β	Model μ	Model σ	Model λ	Model Ω	Model Δ	Model θ	Model π
Ψ - metri c α	0.1904 $\times 10^1$ $\pm \beta \cdot \mu$	0.7143 $\times 10^1$ $\pm \mu \cdot \mu$	0.1679 $\times 10^1$ $\pm \sigma \cdot \mu$	0.7291 $\times 10^2$ $\pm \lambda \cdot \mu$	0.4009 $\times 10^3$ $\pm \Omega \cdot \mu$	0.4325 $\times 10^2$ $\pm \Delta \cdot \mu$	0.6344 $\times 10^2$ $\pm \theta \cdot \mu$	0.5342 $\times 10^1$ $\pm \pi \cdot \mu$	0.2606 $\times 10^3$ $\pm \alpha \cdot \mu$

Ψ- metri c β	0.4615 ×10 ¹ ± μ·μ	0.8669 ×10 ¹ ± σ·μ	0.3841 ×10 ³ ± λ·μ	0.7802 ×10 ³ ± Ω·μ	0.3916 ×10 ¹ ± Δ·μ	0.7421 ×10 ² ± θ·μ	0.9190 ×10 ³ ± π·μ	0.9079 ×10 ¹ ± α·μ	0.3431 ×10 ¹ ± β·μ
Ψ- metri c μ	0.2893 ×10 ³ ± σ·μ	0.3857 ×10 ¹ ± λ·μ	0.6535 ×10 ² ± Ω·μ	0.6018 ×10 ² ± Δ·μ	0.8176 ×10 ³ ± θ·μ	0.7531 ×10 ¹ ± π·μ	0.4806 ×10 ¹ ± α·μ	0.6603 ×10 ¹ ± β·μ	0.2183 ×10 ³ ± μ·μ
Ψ- metri c σ	0.4906 ×10 ² ± λ·μ	0.6483 ×10 ³ ± Ω·μ	0.3289 ×10 ² ± Δ·μ	0.7868 ×10 ³ ± θ·μ	0.8044 ×10 ¹ ± π·μ	0.1739 ×10 ¹ ± α·μ	0.7416 ×10 ³ ± β·μ	0.8307 ×10 ² ± μ·μ	0.7583 ×10 ² ± σ·μ
Ψ- metri c λ	0.6454 ×10 ¹ ± Ω·μ	0.8856 ×10 ¹ ± Δ·μ	0.6781 ×10 ² ± θ·μ	0.8119 ×10 ² ± π·μ	0.9371 ×10 ² ± α·μ	0.7541 ×10 ³ ± β·μ	0.2170 ×10 ² ± μ·μ	0.8672 ×10 ³ ± σ·μ	0.9431 ×10 ² ± λ·μ
Ψ- metri c Ω	0.2988 ×10 ² ± Δ·μ	0.9366 ×10 ² ± θ·μ	0.7309 ×10 ² ± π·μ	0.4529 ×10 ² ± α·μ	0.8948 ×10 ² ± β·μ	0.2516 ×10 ¹ ± μ·μ	0.2967 ×10 ³ ± σ·μ	0.3334 ×10 ¹ ± λ·μ	0.6236 ×10 ² ± Ω·μ
Ψ- metri c Δ	0.8070 ×10 ² ± θ·μ	0.6021 ×10 ¹ ± π·μ	0.3547 ×10 ² ± α·μ	0.3501 ×10 ¹ ± β·μ	0.4022 ×10 ¹ ± μ·μ	0.3300 ×10 ³ ± σ·μ	0.2081 ×10 ² ± λ·μ	0.4869 ×10 ³ ± Ω·μ	0.5725 ×10 ² ± Δ·μ
Ψ- metri c θ	0.5421 ×10 ² ± π·μ	0.7968 ×10 ¹ ± α·μ	0.5856 ×10 ³ ± β·μ	0.6520 ×10 ² ± μ·μ	0.8967 ×10 ³ ± σ·μ	0.3381 ×10 ¹ ± λ·μ	0.5332 ×10 ³ ± Ω·μ	0.2568 ×10 ¹ ± Δ·μ	0.7243 ×10 ³ ± θ·μ
Ψ- metri c π	0.6595 ×10 ³ ± α·μ	0.7580 ×10 ³ ± β·μ	0.5297 ×10 ¹ ± μ·μ	0.6304 ×10 ³ ± σ·μ	0.4364 ×10 ³ ± λ·μ	0.4515 ×10 ³ ± Ω·μ	0.7908 ×10 ³ ± Δ·μ	0.5031 ×10 ¹ ± θ·μ	0.8022 ×10 ¹ ± π·μ

Table 2. Incremental predictive gain following inclusion of mean arterial pressure and uterine artery Doppler indices

Com posite Para meter	Model α	Model β	Model μ	Model σ	Model λ	Model Ω	Model Δ	Model θ	Model π
--------------------------------	------------	------------	------------	------------	------------	------------	------------	------------	------------

JOURNAL OF BIOLOGICAL AND MEDICAL INNOVATIONS

Ψ- metri c α	0.4136 ×10 ³ ± β·μ	0.4241 ×10 ² ± μ·μ	0.4080 ×10 ³ ± σ·μ	0.9179 ×10 ¹ ± λ·μ	0.2656 ×10 ¹ ± Ω·μ	0.1802 ×10 ³ ± Δ·μ	0.2458 ×10 ³ ± θ·μ	0.3959 ×10 ² ± π·μ	0.2417 ×10 ² ± α·μ
Ψ- metri c β	0.3604 ×10 ³ ± μ·μ	0.4089 ×10 ¹ ± σ·μ	0.5092 ×10 ² ± λ·μ	0.2233 ×10 ³ ± Ω·μ	0.5033 ×10 ³ ± Δ·μ	0.3312 ×10 ² ± θ·μ	0.7956 ×10 ¹ ± π·μ	0.5404 ×10 ² ± α·μ	0.3476 ×10 ³ ± β·μ
Ψ- metri c μ	0.3124 ×10 ² ± σ·μ	0.2949 ×10 ³ ± λ·μ	0.3850 ×10 ² ± Ω·μ	0.2776 ×10 ² ± Δ·μ	0.5975 ×10 ² ± θ·μ	0.6351 ×10 ³ ± π·μ	0.3774 ×10 ¹ ± α·μ	0.6094 ×10 ³ ± β·μ	0.9483 ×10 ² ± μ·μ
Ψ- metri c σ	0.7302 ×10 ³ ± λ·μ	0.5547 ×10 ¹ ± Ω·μ	0.1795 ×10 ³ ± Δ·μ	0.9339 ×10 ¹ ± θ·μ	0.8506 ×10 ² ± π·μ	0.9593 ×10 ³ ± α·μ	0.9355 ×10 ² ± β·μ	0.9540 ×10 ² ± μ·μ	0.9396 ×10 ² ± σ·μ
Ψ- metri c λ	0.4555 ×10 ² ± Ω·μ	0.7784 ×10 ³ ± Δ·μ	0.3109 ×10 ³ ± θ·μ	0.3381 ×10 ³ ± π·μ	0.2449 ×10 ³ ± α·μ	0.2393 ×10 ¹ ± β·μ	0.2358 ×10 ² ± μ·μ	0.6388 ×10 ² ± σ·μ	0.7970 ×10 ² ± λ·μ
Ψ- metri c Ω	0.4785 ×10 ² ± Δ·μ	0.2769 ×10 ¹ ± θ·μ	0.6821 ×10 ² ± π·μ	0.2349 ×10 ¹ ± α·μ	0.9086 ×10 ² ± β·μ	0.9712 ×10 ¹ ± μ·μ	0.2026 ×10 ³ ± σ·μ	0.8661 ×10 ¹ ± λ·μ	0.3959 ×10 ² ± Ω·μ
Ψ- metri c Δ	0.8638 ×10 ¹ ± θ·μ	0.7552 ×10 ³ ± π·μ	0.5722 ×10 ² ± α·μ	0.5109 ×10 ² ± β·μ	0.2243 ×10 ¹ ± μ·μ	0.2275 ×10 ² ± σ·μ	0.7563 ×10 ³ ± λ·μ	0.4593 ×10 ³ ± Ω·μ	0.3739 ×10 ³ ± Δ·μ
Ψ- metri c θ	0.5712 ×10 ¹ ± π·μ	0.7661 ×10 ³ ± α·μ	0.9558 ×10 ² ± β·μ	0.9744 ×10 ³ ± μ·μ	0.6695 ×10 ³ ± σ·μ	0.1862 ×10 ¹ ± λ·μ	0.9272 ×10 ² ± Ω·μ	0.4786 ×10 ² ± Δ·μ	0.4488 ×10 ² ± θ·μ
Ψ- metri c π	0.8941 ×10 ² ± α·μ	0.4968 ×10 ² ± β·μ	0.9134 ×10 ³ ± μ·μ	0.4963 ×10 ¹ ± σ·μ	0.1850 ×10 ³ ± λ·μ	0.6420 ×10 ³ ± Ω·μ	0.8926 ×10 ² ± Δ·μ	0.9021 ×10 ¹ ± θ·μ	0.3262 ×10 ² ± π·μ

Table 3. Comparative sensitivity shifts after integration of placental growth factor with μ -scaled adjustment

Com posite Para meter	Model α	Model β	Model μ	Model σ	Model λ	Model Ω	Model Δ	Model θ	Model π
Ψ - metri c α	0.1731 $\times 10^3$ $\pm \beta \cdot \mu$	0.5776 $\times 10^3$ $\pm \mu \cdot \mu$	0.9022 $\times 10^3$ $\pm \sigma \cdot \mu$	0.1833 $\times 10^3$ $\pm \lambda \cdot \mu$	0.3345 $\times 10^2$ $\pm \Omega \cdot \mu$	0.7142 $\times 10^3$ $\pm \Delta \cdot \mu$	0.5745 $\times 10^1$ $\pm \theta \cdot \mu$	0.6404 $\times 10^2$ $\pm \pi \cdot \mu$	0.7340 $\times 10^3$ $\pm \alpha \cdot \mu$
Ψ - metri c β	0.3018 $\times 10^1$ $\pm \mu \cdot \mu$	0.5214 $\times 10^1$ $\pm \sigma \cdot \mu$	0.3753 $\times 10^1$ $\pm \lambda \cdot \mu$	0.6522 $\times 10^3$ $\pm \Omega \cdot \mu$	0.7754 $\times 10^3$ $\pm \Delta \cdot \mu$	0.7362 $\times 10^1$ $\pm \theta \cdot \mu$	0.4249 $\times 10^1$ $\pm \pi \cdot \mu$	0.7246 $\times 10^2$ $\pm \alpha \cdot \mu$	0.1804 $\times 10^2$ $\pm \beta \cdot \mu$
Ψ - metri c μ	0.8226 $\times 10^3$ $\pm \sigma \cdot \mu$	0.8655 $\times 10^3$ $\pm \lambda \cdot \mu$	0.5673 $\times 10^2$ $\pm \Omega \cdot \mu$	0.8825 $\times 10^3$ $\pm \Delta \cdot \mu$	0.6364 $\times 10^2$ $\pm \theta \cdot \mu$	0.7824 $\times 10^2$ $\pm \pi \cdot \mu$	0.1541 $\times 10^2$ $\pm \alpha \cdot \mu$	0.2815 $\times 10^1$ $\pm \beta \cdot \mu$	0.3095 $\times 10^1$ $\pm \mu \cdot \mu$
Ψ - metri c σ	0.5581 $\times 10^1$ $\pm \lambda \cdot \mu$	0.4517 $\times 10^1$ $\pm \Omega \cdot \mu$	0.5085 $\times 10^2$ $\pm \Delta \cdot \mu$	0.7873 $\times 10^2$ $\pm \theta \cdot \mu$	0.8173 $\times 10^2$ $\pm \pi \cdot \mu$	0.2069 $\times 10^3$ $\pm \alpha \cdot \mu$	0.4261 $\times 10^2$ $\pm \beta \cdot \mu$	0.6508 $\times 10^2$ $\pm \mu \cdot \mu$	0.7183 $\times 10^1$ $\pm \sigma \cdot \mu$
Ψ - metri c λ	0.8539 $\times 10^1$ $\pm \Omega \cdot \mu$	0.7727 $\times 10^1$ $\pm \Delta \cdot \mu$	0.2146 $\times 10^2$ $\pm \theta \cdot \mu$	0.7797 $\times 10^2$ $\pm \pi \cdot \mu$	0.7108 $\times 10^1$ $\pm \alpha \cdot \mu$	0.7404 $\times 10^2$ $\pm \beta \cdot \mu$	0.5139 $\times 10^2$ $\pm \mu \cdot \mu$	0.9483 $\times 10^3$ $\pm \sigma \cdot \mu$	0.4864 $\times 10^1$ $\pm \lambda \cdot \mu$
Ψ - metri c Ω	0.2509 $\times 10^2$ $\pm \Delta \cdot \mu$	0.4394 $\times 10^3$ $\pm \theta \cdot \mu$	0.4553 $\times 10^2$ $\pm \pi \cdot \mu$	0.9152 $\times 10^2$ $\pm \alpha \cdot \mu$	0.8948 $\times 10^2$ $\pm \beta \cdot \mu$	0.1879 $\times 10^1$ $\pm \mu \cdot \mu$	0.3822 $\times 10^1$ $\pm \sigma \cdot \mu$	0.5880 $\times 10^3$ $\pm \lambda \cdot \mu$	0.1509 $\times 10^1$ $\pm \Omega \cdot \mu$
Ψ - metri c Δ	0.7019 $\times 10^1$ $\pm \theta \cdot \mu$	0.4234 $\times 10^2$ $\pm \pi \cdot \mu$	0.3193 $\times 10^3$ $\pm \alpha \cdot \mu$	0.7453 $\times 10^3$ $\pm \beta \cdot \mu$	0.2897 $\times 10^1$ $\pm \mu \cdot \mu$	0.9336 $\times 10^3$ $\pm \sigma \cdot \mu$	0.4132 $\times 10^2$ $\pm \lambda \cdot \mu$	0.9625 $\times 10^2$ $\pm \Omega \cdot \mu$	0.9157 $\times 10^2$ $\pm \Delta \cdot \mu$
Ψ - metri c θ	0.5875 $\times 10^1$ $\pm \pi \cdot \mu$	0.8951 $\times 10^1$ $\pm \alpha \cdot \mu$	0.9498 $\times 10^1$ $\pm \beta \cdot \mu$	0.4533 $\times 10^1$ $\pm \mu \cdot \mu$	0.2359 $\times 10^3$ $\pm \sigma \cdot \mu$	0.9258 $\times 10^1$ $\pm \lambda \cdot \mu$	0.9016 $\times 10^1$ $\pm \Omega \cdot \mu$	0.9132 $\times 10^3$ $\pm \Delta \cdot \mu$	0.7691 $\times 10^2$ $\pm \theta \cdot \mu$
Ψ - metri c π	0.4587 $\times 10^2$ $\pm \alpha \cdot \mu$	0.7762 $\times 10^2$ $\pm \beta \cdot \mu$	0.3188 $\times 10^2$ $\pm \mu \cdot \mu$	0.3987 $\times 10^2$ $\pm \sigma \cdot \mu$	0.5451 $\times 10^3$ $\pm \lambda \cdot \mu$	0.9120 $\times 10^2$ $\pm \Omega \cdot \mu$	0.3223 $\times 10^1$ $\pm \Delta \cdot \mu$	0.6041 $\times 10^3$ $\pm \theta \cdot \mu$	0.6961 $\times 10^2$ $\pm \pi \cdot \mu$

Table 4. Variance attenuation effects observed after incorporation of sFlt-1–PlGF ratio dynamics

Composite Parameter	Model α	Model β	Model μ	Model σ	Model λ	Model Ω	Model Δ	Model θ	Model π
Ψ -metri c α	0.9598 $\times 10^3$ $\pm \beta \cdot \mu$	0.7619 $\times 10^1$ $\pm \mu \cdot \mu$	0.3453 $\times 10^3$ $\pm \sigma \cdot \mu$	0.2398 $\times 10^2$ $\pm \lambda \cdot \mu$	0.8509 $\times 10^2$ $\pm \Omega \cdot \mu$	0.4357 $\times 10^1$ $\pm \Delta \cdot \mu$	0.2075 $\times 10^2$ $\pm \theta \cdot \mu$	0.7936 $\times 10^3$ $\pm \pi \cdot \mu$	0.9788 $\times 10^1$ $\pm \alpha \cdot \mu$
Ψ -metri c β	0.9572 $\times 10^1$ $\pm \mu \cdot \mu$	0.4243 $\times 10^2$ $\pm \sigma \cdot \mu$	0.3186 $\times 10^3$ $\pm \lambda \cdot \mu$	0.1994 $\times 10^1$ $\pm \Omega \cdot \mu$	0.7932 $\times 10^1$ $\pm \Delta \cdot \mu$	0.1582 $\times 10^1$ $\pm \theta \cdot \mu$	0.6630 $\times 10^2$ $\pm \pi \cdot \mu$	0.9588 $\times 10^1$ $\pm \alpha \cdot \mu$	0.9049 $\times 10^2$ $\pm \beta \cdot \mu$
Ψ -metri c μ	0.1955 $\times 10^1$ $\pm \sigma \cdot \mu$	0.7648 $\times 10^2$ $\pm \lambda \cdot \mu$	0.2013 $\times 10^3$ $\pm \Omega \cdot \mu$	0.7122 $\times 10^3$ $\pm \Delta \cdot \mu$	0.8428 $\times 10^3$ $\pm \theta \cdot \mu$	0.8039 $\times 10^1$ $\pm \pi \cdot \mu$	0.4168 $\times 10^1$ $\pm \alpha \cdot \mu$	0.8984 $\times 10^1$ $\pm \beta \cdot \mu$	0.8322 $\times 10^2$ $\pm \mu \cdot \mu$
Ψ -metri c σ	0.3237 $\times 10^2$ $\pm \lambda \cdot \mu$	0.9538 $\times 10^3$ $\pm \Omega \cdot \mu$	0.3913 $\times 10^2$ $\pm \Delta \cdot \mu$	0.1610 $\times 10^3$ $\pm \theta \cdot \mu$	0.2359 $\times 10^3$ $\pm \pi \cdot \mu$	0.6481 $\times 10^1$ $\pm \alpha \cdot \mu$	0.9715 $\times 10^2$ $\pm \beta \cdot \mu$	0.2249 $\times 10^2$ $\pm \mu \cdot \mu$	0.3113 $\times 10^1$ $\pm \sigma \cdot \mu$
Ψ -metri c λ	0.3993 $\times 10^3$ $\pm \Omega \cdot \mu$	0.2371 $\times 10^3$ $\pm \Delta \cdot \mu$	0.8093 $\times 10^1$ $\pm \theta \cdot \mu$	0.4570 $\times 10^3$ $\pm \pi \cdot \mu$	0.2231 $\times 10^3$ $\pm \alpha \cdot \mu$	0.4429 $\times 10^2$ $\pm \beta \cdot \mu$	0.5081 $\times 10^2$ $\pm \mu \cdot \mu$	0.3246 $\times 10^1$ $\pm \sigma \cdot \mu$	0.6741 $\times 10^1$ $\pm \lambda \cdot \mu$
Ψ -metri c Ω	0.7914 $\times 10^3$ $\pm \Delta \cdot \mu$	0.3188 $\times 10^3$ $\pm \theta \cdot \mu$	0.2900 $\times 10^1$ $\pm \pi \cdot \mu$	0.4957 $\times 10^1$ $\pm \alpha \cdot \mu$	0.6652 $\times 10^1$ $\pm \beta \cdot \mu$	0.2309 $\times 10^2$ $\pm \mu \cdot \mu$	0.7788 $\times 10^1$ $\pm \sigma \cdot \mu$	0.3056 $\times 10^1$ $\pm \lambda \cdot \mu$	0.2263 $\times 10^1$ $\pm \Omega \cdot \mu$
Ψ -metri c Δ	0.4423 $\times 10^1$ $\pm \theta \cdot \mu$	0.5634 $\times 10^2$ $\pm \pi \cdot \mu$	0.9021 $\times 10^1$ $\pm \alpha \cdot \mu$	0.5874 $\times 10^3$ $\pm \beta \cdot \mu$	0.5256 $\times 10^1$ $\pm \mu \cdot \mu$	0.1896 $\times 10^1$ $\pm \sigma \cdot \mu$	0.7456 $\times 10^2$ $\pm \lambda \cdot \mu$	0.3394 $\times 10^2$ $\pm \Omega \cdot \mu$	0.4614 $\times 10^1$ $\pm \Delta \cdot \mu$
Ψ -metri c θ	0.5302 $\times 10^2$ $\pm \pi \cdot \mu$	0.6852 $\times 10^1$ $\pm \alpha \cdot \mu$	0.4361 $\times 10^2$ $\pm \beta \cdot \mu$	0.1646 $\times 10^1$ $\pm \mu \cdot \mu$	0.4524 $\times 10^2$ $\pm \sigma \cdot \mu$	0.5910 $\times 10^3$ $\pm \lambda \cdot \mu$	0.9684 $\times 10^1$ $\pm \Omega \cdot \mu$	0.4947 $\times 10^2$ $\pm \Delta \cdot \mu$	0.4947 $\times 10^3$ $\pm \theta \cdot \mu$

Ψ - metri $c \pi$	0.7493 $\times 10^3$ $\pm \alpha \cdot \mu$	0.6410 $\times 10^1$ $\pm \beta \cdot \mu$	0.8284 $\times 10^1$ $\pm \mu \cdot \mu$	0.7408 $\times 10^1$ $\pm \sigma \cdot \mu$	0.6678 $\times 10^3$ $\pm \lambda \cdot \mu$	0.4550 $\times 10^3$ $\pm \Omega \cdot \mu$	0.6085 $\times 10^3$ $\pm \Delta \cdot \mu$	0.3586 $\times 10^2$ $\pm \theta \cdot \mu$	0.8273 $\times 10^2$ $\pm \pi \cdot \mu$
------------------------------	---	--	--	---	--	---	---	---	--

Table 5. Multimodal fusion outcomes combining biochemical and biophysical predictors using Δ -modulated weighting

Com posite Para meter	Model α	Model β	Model μ	Model σ	Model λ	Model Ω	Model Δ	Model θ	Model π
Ψ - metri $c \alpha$	0.1948 $\times 10^1$ $\pm \beta \cdot \mu$	0.7378 $\times 10^1$ $\pm \mu \cdot \mu$	0.1952 $\times 10^1$ $\pm \sigma \cdot \mu$	0.6067 $\times 10^3$ $\pm \lambda \cdot \mu$	0.2344 $\times 10^2$ $\pm \Omega \cdot \mu$	0.2684 $\times 10^3$ $\pm \Delta \cdot \mu$	0.6936 $\times 10^3$ $\pm \theta \cdot \mu$	0.8793 $\times 10^2$ $\pm \pi \cdot \mu$	0.7958 $\times 10^1$ $\pm \alpha \cdot \mu$
Ψ - metri $c \beta$	0.3147 $\times 10^1$ $\pm \mu \cdot \mu$	0.7597 $\times 10^1$ $\pm \sigma \cdot \mu$	0.7377 $\times 10^1$ $\pm \lambda \cdot \mu$	0.6196 $\times 10^2$ $\pm \Omega \cdot \mu$	0.7520 $\times 10^1$ $\pm \Delta \cdot \mu$	0.4052 $\times 10^3$ $\pm \theta \cdot \mu$	0.7660 $\times 10^2$ $\pm \pi \cdot \mu$	0.2722 $\times 10^1$ $\pm \alpha \cdot \mu$	0.7609 $\times 10^1$ $\pm \beta \cdot \mu$
Ψ - metri $c \mu$	0.8641 $\times 10^2$ $\pm \sigma \cdot \mu$	0.6529 $\times 10^3$ $\pm \lambda \cdot \mu$	0.3599 $\times 10^1$ $\pm \Omega \cdot \mu$	0.8157 $\times 10^2$ $\pm \Delta \cdot \mu$	0.3536 $\times 10^2$ $\pm \theta \cdot \mu$	0.9581 $\times 10^2$ $\pm \pi \cdot \mu$	0.5150 $\times 10^2$ $\pm \alpha \cdot \mu$	0.6373 $\times 10^3$ $\pm \beta \cdot \mu$	0.7494 $\times 10^1$ $\pm \mu \cdot \mu$
Ψ - metri $c \sigma$	0.2036 $\times 10^3$ $\pm \lambda \cdot \mu$	0.2629 $\times 10^3$ $\pm \Omega \cdot \mu$	0.5526 $\times 10^2$ $\pm \Delta \cdot \mu$	0.6874 $\times 10^3$ $\pm \theta \cdot \mu$	0.5882 $\times 10^1$ $\pm \pi \cdot \mu$	0.7200 $\times 10^1$ $\pm \alpha \cdot \mu$	0.4854 $\times 10^3$ $\pm \beta \cdot \mu$	0.7318 $\times 10^2$ $\pm \mu \cdot \mu$	0.3496 $\times 10^2$ $\pm \sigma \cdot \mu$
Ψ - metri $c \lambda$	0.7971 $\times 10^2$ $\pm \Omega \cdot \mu$	0.5055 $\times 10^3$ $\pm \Delta \cdot \mu$	0.3671 $\times 10^3$ $\pm \theta \cdot \mu$	0.2753 $\times 10^1$ $\pm \pi \cdot \mu$	0.5731 $\times 10^3$ $\pm \alpha \cdot \mu$	0.5517 $\times 10^2$ $\pm \beta \cdot \mu$	0.2480 $\times 10^1$ $\pm \mu \cdot \mu$	0.4131 $\times 10^2$ $\pm \sigma \cdot \mu$	0.4908 $\times 10^1$ $\pm \lambda \cdot \mu$
Ψ - metri $c \Omega$	0.6299 $\times 10^3$ $\pm \Delta \cdot \mu$	0.3618 $\times 10^2$ $\pm \theta \cdot \mu$	0.2458 $\times 10^1$ $\pm \pi \cdot \mu$	0.9588 $\times 10^2$ $\pm \alpha \cdot \mu$	0.4488 $\times 10^1$ $\pm \beta \cdot \mu$	0.1604 $\times 10^1$ $\pm \mu \cdot \mu$	0.6533 $\times 10^1$ $\pm \sigma \cdot \mu$	0.6057 $\times 10^1$ $\pm \lambda \cdot \mu$	0.6974 $\times 10^3$ $\pm \Omega \cdot \mu$
Ψ - metri $c \Delta$	0.8589 $\times 10^1$ $\pm \theta \cdot \mu$	0.2072 $\times 10^2$ $\pm \pi \cdot \mu$	0.8931 $\times 10^1$ $\pm \alpha \cdot \mu$	0.4574 $\times 10^2$ $\pm \beta \cdot \mu$	0.2740 $\times 10^2$ $\pm \mu \cdot \mu$	0.8552 $\times 10^2$ $\pm \sigma \cdot \mu$	0.5183 $\times 10^2$ $\pm \lambda \cdot \mu$	0.4077 $\times 10^3$ $\pm \Omega \cdot \mu$	0.6638 $\times 10^2$ $\pm \Delta \cdot \mu$

Ψ - metri c θ	0.4331 $\times 10^3$ $\pm \pi \cdot \mu$	0.2869 $\times 10^1$ $\pm \alpha \cdot \mu$	0.4892 $\times 10^2$ $\pm \beta \cdot \mu$	0.7836 $\times 10^3$ $\pm \mu \cdot \mu$	0.5673 $\times 10^3$ $\pm \sigma \cdot \mu$	0.9451 $\times 10^2$ $\pm \lambda \cdot \mu$	0.8476 $\times 10^2$ $\pm \Omega \cdot \mu$	0.9466 $\times 10^2$ $\pm \Delta \cdot \mu$	0.6665 $\times 10^1$ $\pm \theta \cdot \mu$
Ψ - metri c π	0.2126 $\times 10^3$ $\pm \alpha \cdot \mu$	0.5949 $\times 10^2$ $\pm \beta \cdot \mu$	0.9549 $\times 10^3$ $\pm \mu \cdot \mu$	0.3123 $\times 10^3$ $\pm \sigma \cdot \mu$	0.2510 $\times 10^3$ $\pm \lambda \cdot \mu$	0.5020 $\times 10^2$ $\pm \Omega \cdot \mu$	0.8380 $\times 10^1$ $\pm \Delta \cdot \mu$	0.7138 $\times 10^3$ $\pm \theta \cdot \mu$	0.6513 $\times 10^2$ $\pm \pi \cdot \mu$

Table 6. Calibration stability of Bayesian posterior risk estimates across σ -regularized models

Com posite Para meter	Model α	Model β	Model μ	Model σ	Model λ	Model Ω	Model Δ	Model θ	Model π
Ψ - metri c α	0.4983 $\times 10^2$ $\pm \beta \cdot \mu$	0.2397 $\times 10^3$ $\pm \mu \cdot \mu$	0.2127 $\times 10^3$ $\pm \sigma \cdot \mu$	0.8069 $\times 10^2$ $\pm \lambda \cdot \mu$	0.5571 $\times 10^3$ $\pm \Omega \cdot \mu$	0.4928 $\times 10^3$ $\pm \Delta \cdot \mu$	0.6303 $\times 10^2$ $\pm \theta \cdot \mu$	0.2084 $\times 10^3$ $\pm \pi \cdot \mu$	0.6541 $\times 10^2$ $\pm \alpha \cdot \mu$
Ψ - metri c β	0.8078 $\times 10^3$ $\pm \mu \cdot \mu$	0.3258 $\times 10^3$ $\pm \sigma \cdot \mu$	0.1590 $\times 10^2$ $\pm \lambda \cdot \mu$	0.5195 $\times 10^1$ $\pm \Omega \cdot \mu$	0.3799 $\times 10^2$ $\pm \Delta \cdot \mu$	0.9218 $\times 10^3$ $\pm \theta \cdot \mu$	0.2265 $\times 10^3$ $\pm \pi \cdot \mu$	0.9755 $\times 10^2$ $\pm \alpha \cdot \mu$	0.9329 $\times 10^3$ $\pm \beta \cdot \mu$
Ψ - metri c μ	0.4877 $\times 10^1$ $\pm \sigma \cdot \mu$	0.5567 $\times 10^2$ $\pm \lambda \cdot \mu$	0.6730 $\times 10^2$ $\pm \Omega \cdot \mu$	0.2883 $\times 10^2$ $\pm \Delta \cdot \mu$	0.2326 $\times 10^2$ $\pm \theta \cdot \mu$	0.3417 $\times 10^2$ $\pm \pi \cdot \mu$	0.4521 $\times 10^2$ $\pm \alpha \cdot \mu$	0.8937 $\times 10^2$ $\pm \beta \cdot \mu$	0.7998 $\times 10^2$ $\pm \mu \cdot \mu$
Ψ - metri c σ	0.9354 $\times 10^1$ $\pm \lambda \cdot \mu$	0.6244 $\times 10^3$ $\pm \Omega \cdot \mu$	0.9016 $\times 10^3$ $\pm \Delta \cdot \mu$	0.6022 $\times 10^1$ $\pm \theta \cdot \mu$	0.8647 $\times 10^2$ $\pm \pi \cdot \mu$	0.4197 $\times 10^3$ $\pm \alpha \cdot \mu$	0.1579 $\times 10^1$ $\pm \beta \cdot \mu$	0.5198 $\times 10^3$ $\pm \mu \cdot \mu$	0.3381 $\times 10^2$ $\pm \sigma \cdot \mu$
Ψ - metri c λ	0.8553 $\times 10^3$ $\pm \Omega \cdot \mu$	0.9252 $\times 10^2$ $\pm \Delta \cdot \mu$	0.2162 $\times 10^2$ $\pm \theta \cdot \mu$	0.3485 $\times 10^1$ $\pm \pi \cdot \mu$	0.3362 $\times 10^2$ $\pm \alpha \cdot \mu$	0.9142 $\times 10^2$ $\pm \beta \cdot \mu$	0.6117 $\times 10^2$ $\pm \mu \cdot \mu$	0.3524 $\times 10^2$ $\pm \sigma \cdot \mu$	0.9768 $\times 10^2$ $\pm \lambda \cdot \mu$
Ψ - metri c Ω	0.7050 $\times 10^1$ $\pm \Delta \cdot \mu$	0.3435 $\times 10^3$ $\pm \theta \cdot \mu$	0.3317 $\times 10^1$ $\pm \pi \cdot \mu$	0.7523 $\times 10^3$ $\pm \alpha \cdot \mu$	0.5612 $\times 10^2$ $\pm \beta \cdot \mu$	0.1867 $\times 10^2$ $\pm \mu \cdot \mu$	0.8337 $\times 10^1$ $\pm \sigma \cdot \mu$	0.4935 $\times 10^3$ $\pm \lambda \cdot \mu$	0.8862 $\times 10^1$ $\pm \Omega \cdot \mu$

Ψ - metri c Δ	0.2270 $\times 10^3$ $\pm \theta \cdot \mu$	0.3497 $\times 10^2$ $\pm \pi \cdot \mu$	0.2280 $\times 10^3$ $\pm \alpha \cdot \mu$	0.6126 $\times 10^3$ $\pm \beta \cdot \mu$	0.3368 $\times 10^2$ $\pm \mu \cdot \mu$	0.5455 $\times 10^1$ $\pm \sigma \cdot \mu$	0.4538 $\times 10^3$ $\pm \lambda \cdot \mu$	0.8841 $\times 10^3$ $\pm \Omega \cdot \mu$	0.4529 $\times 10^3$ $\pm \Delta \cdot \mu$
Ψ - metri c θ	0.1769 $\times 10^3$ $\pm \pi \cdot \mu$	0.3225 $\times 10^2$ $\pm \alpha \cdot \mu$	0.8384 $\times 10^1$ $\pm \beta \cdot \mu$	0.5698 $\times 10^2$ $\pm \mu \cdot \mu$	0.6305 $\times 10^3$ $\pm \sigma \cdot \mu$	0.8138 $\times 10^2$ $\pm \lambda \cdot \mu$	0.8444 $\times 10^2$ $\pm \Omega \cdot \mu$	0.7387 $\times 10^2$ $\pm \Delta \cdot \mu$	0.4409 $\times 10^1$ $\pm \theta \cdot \mu$
Ψ - metri c π	0.2896 $\times 10^2$ $\pm \alpha \cdot \mu$	0.8869 $\times 10^1$ $\pm \beta \cdot \mu$	0.3682 $\times 10^1$ $\pm \mu \cdot \mu$	0.6732 $\times 10^3$ $\pm \sigma \cdot \mu$	0.2094 $\times 10^2$ $\pm \lambda \cdot \mu$	0.9469 $\times 10^2$ $\pm \Omega \cdot \mu$	0.8452 $\times 10^3$ $\pm \Delta \cdot \mu$	0.6207 $\times 10^2$ $\pm \theta \cdot \mu$	0.5582 $\times 10^3$ $\pm \pi \cdot \mu$

Table 7. Reduction in false-positive propagation following λ -constrained composite modeling

Com posite Para meter	Model α	Model β	Model μ	Model σ	Model λ	Model Ω	Model Δ	Model θ	Model π
Ψ - metri c α	0.5597 $\times 10^1$ $\pm \beta \cdot \mu$	0.3526 $\times 10^3$ $\pm \mu \cdot \mu$	0.5373 $\times 10^1$ $\pm \sigma \cdot \mu$	0.8856 $\times 10^1$ $\pm \lambda \cdot \mu$	0.2161 $\times 10^3$ $\pm \Omega \cdot \mu$	0.4755 $\times 10^3$ $\pm \Delta \cdot \mu$	0.5317 $\times 10^3$ $\pm \theta \cdot \mu$	0.3018 $\times 10^2$ $\pm \pi \cdot \mu$	0.3683 $\times 10^1$ $\pm \alpha \cdot \mu$
Ψ - metri c β	0.7110 $\times 10^2$ $\pm \mu \cdot \mu$	0.2143 $\times 10^1$ $\pm \sigma \cdot \mu$	0.6511 $\times 10^2$ $\pm \lambda \cdot \mu$	0.3701 $\times 10^3$ $\pm \Omega \cdot \mu$	0.3088 $\times 10^1$ $\pm \Delta \cdot \mu$	0.1830 $\times 10^3$ $\pm \theta \cdot \mu$	0.9791 $\times 10^2$ $\pm \pi \cdot \mu$	0.8783 $\times 10^2$ $\pm \alpha \cdot \mu$	0.3225 $\times 10^1$ $\pm \beta \cdot \mu$
Ψ - metri c μ	0.9699 $\times 10^3$ $\pm \sigma \cdot \mu$	0.4795 $\times 10^1$ $\pm \lambda \cdot \mu$	0.2133 $\times 10^3$ $\pm \Omega \cdot \mu$	0.9711 $\times 10^3$ $\pm \Delta \cdot \mu$	0.3423 $\times 10^1$ $\pm \theta \cdot \mu$	0.6191 $\times 10^1$ $\pm \pi \cdot \mu$	0.7387 $\times 10^1$ $\pm \alpha \cdot \mu$	0.4733 $\times 10^3$ $\pm \beta \cdot \mu$	0.5973 $\times 10^3$ $\pm \mu \cdot \mu$
Ψ - metri c σ	0.3041 $\times 10^1$ $\pm \lambda \cdot \mu$	0.6244 $\times 10^1$ $\pm \Omega \cdot \mu$	0.2013 $\times 10^1$ $\pm \Delta \cdot \mu$	0.8995 $\times 10^2$ $\pm \theta \cdot \mu$	0.4542 $\times 10^2$ $\pm \pi \cdot \mu$	0.2611 $\times 10^2$ $\pm \alpha \cdot \mu$	0.5879 $\times 10^1$ $\pm \beta \cdot \mu$	0.3867 $\times 10^1$ $\pm \mu \cdot \mu$	0.6109 $\times 10^2$ $\pm \sigma \cdot \mu$
Ψ - metri c λ	0.5271 $\times 10^1$ $\pm \Omega \cdot \mu$	0.3524 $\times 10^2$ $\pm \Delta \cdot \mu$	0.7335 $\times 10^1$ $\pm \theta \cdot \mu$	0.1605 $\times 10^2$ $\pm \pi \cdot \mu$	0.3889 $\times 10^3$ $\pm \alpha \cdot \mu$	0.1591 $\times 10^1$ $\pm \beta \cdot \mu$	0.8377 $\times 10^1$ $\pm \mu \cdot \mu$	0.8904 $\times 10^1$ $\pm \sigma \cdot \mu$	0.5623 $\times 10^2$ $\pm \lambda \cdot \mu$

Ψ - metri c Ω	0.4265 $\times 10^1$ $\pm \Delta \cdot \mu$	0.7736 $\times 10^3$ $\pm \theta \cdot \mu$	0.6815 $\times 10^1$ $\pm \pi \cdot \mu$	0.6204 $\times 10^2$ $\pm \alpha \cdot \mu$	0.6345 $\times 10^1$ $\pm \beta \cdot \mu$	0.3994 $\times 10^1$ $\pm \mu \cdot \mu$	0.1623 $\times 10^3$ $\pm \sigma \cdot \mu$	0.5265 $\times 10^3$ $\pm \lambda \cdot \mu$	0.6842 $\times 10^1$ $\pm \Omega \cdot \mu$
Ψ - metri c Δ	0.4401 $\times 10^3$ $\pm \theta \cdot \mu$	0.1552 $\times 10^2$ $\pm \pi \cdot \mu$	0.9506 $\times 10^2$ $\pm \alpha \cdot \mu$	0.9158 $\times 10^2$ $\pm \beta \cdot \mu$	0.7565 $\times 10^3$ $\pm \mu \cdot \mu$	0.2471 $\times 10^2$ $\pm \sigma \cdot \mu$	0.2090 $\times 10^1$ $\pm \lambda \cdot \mu$	0.8267 $\times 10^1$ $\pm \Omega \cdot \mu$	0.8904 $\times 10^2$ $\pm \Delta \cdot \mu$
Ψ - metri c θ	0.3584 $\times 10^1$ $\pm \pi \cdot \mu$	0.8445 $\times 10^1$ $\pm \alpha \cdot \mu$	0.6862 $\times 10^2$ $\pm \beta \cdot \mu$	0.7091 $\times 10^3$ $\pm \mu \cdot \mu$	0.9436 $\times 10^3$ $\pm \sigma \cdot \mu$	0.6135 $\times 10^1$ $\pm \lambda \cdot \mu$	0.8072 $\times 10^3$ $\pm \Omega \cdot \mu$	0.4584 $\times 10^3$ $\pm \Delta \cdot \mu$	0.8389 $\times 10^2$ $\pm \theta \cdot \mu$
Ψ - metri c π	0.9479 $\times 10^2$ $\pm \alpha \cdot \mu$	0.7732 $\times 10^2$ $\pm \beta \cdot \mu$	0.3244 $\times 10^3$ $\pm \mu \cdot \mu$	0.3170 $\times 10^3$ $\pm \sigma \cdot \mu$	0.7376 $\times 10^1$ $\pm \lambda \cdot \mu$	0.9165 $\times 10^2$ $\pm \Omega \cdot \mu$	0.7535 $\times 10^3$ $\pm \Delta \cdot \mu$	0.8909 $\times 10^2$ $\pm \theta \cdot \mu$	0.6023 $\times 10^1$ $\pm \pi \cdot \mu$

Table 8. Cross-model robustness assessment using θ -corrected multidimensional indices

Com posite Para meter	Model α	Model β	Model μ	Model σ	Model λ	Model Ω	Model Δ	Model θ	Model π
Ψ - metri c α	0.7200 $\times 10^3$ $\pm \beta \cdot \mu$	0.8433 $\times 10^1$ $\pm \mu \cdot \mu$	0.9203 $\times 10^1$ $\pm \sigma \cdot \mu$	0.2529 $\times 10^2$ $\pm \lambda \cdot \mu$	0.9614 $\times 10^2$ $\pm \Omega \cdot \mu$	0.8437 $\times 10^1$ $\pm \Delta \cdot \mu$	0.8874 $\times 10^1$ $\pm \theta \cdot \mu$	0.9637 $\times 10^1$ $\pm \pi \cdot \mu$	0.6885 $\times 10^1$ $\pm \alpha \cdot \mu$
Ψ - metri c β	0.6851 $\times 10^1$ $\pm \mu \cdot \mu$	0.2871 $\times 10^2$ $\pm \sigma \cdot \mu$	0.8646 $\times 10^2$ $\pm \lambda \cdot \mu$	0.6475 $\times 10^3$ $\pm \Omega \cdot \mu$	0.9660 $\times 10^1$ $\pm \Delta \cdot \mu$	0.7520 $\times 10^3$ $\pm \theta \cdot \mu$	0.2716 $\times 10^2$ $\pm \pi \cdot \mu$	0.6936 $\times 10^3$ $\pm \alpha \cdot \mu$	0.1539 $\times 10^3$ $\pm \beta \cdot \mu$
Ψ - metri c μ	0.9437 $\times 10^1$ $\pm \sigma \cdot \mu$	0.3853 $\times 10^3$ $\pm \lambda \cdot \mu$	0.9563 $\times 10^1$ $\pm \Omega \cdot \mu$	0.9605 $\times 10^2$ $\pm \Delta \cdot \mu$	0.6872 $\times 10^1$ $\pm \theta \cdot \mu$	0.8024 $\times 10^3$ $\pm \pi \cdot \mu$	0.7900 $\times 10^1$ $\pm \alpha \cdot \mu$	0.8149 $\times 10^3$ $\pm \beta \cdot \mu$	0.6431 $\times 10^3$ $\pm \mu \cdot \mu$
Ψ - metri c σ	0.5901 $\times 10^2$ $\pm \lambda \cdot \mu$	0.4755 $\times 10^2$ $\pm \Omega \cdot \mu$	0.5082 $\times 10^2$ $\pm \Delta \cdot \mu$	0.7610 $\times 10^3$ $\pm \theta \cdot \mu$	0.5697 $\times 10^3$ $\pm \pi \cdot \mu$	0.4893 $\times 10^2$ $\pm \alpha \cdot \mu$	0.2021 $\times 10^3$ $\pm \beta \cdot \mu$	0.7286 $\times 10^3$ $\pm \mu \cdot \mu$	0.8932 $\times 10^2$ $\pm \sigma \cdot \mu$

Ψ- metri c λ	0.3623 ×10 ² ± Ω·μ	0.1896 ×10 ¹ ± Δ·μ	0.8239 ×10 ² ± θ·μ	0.8387 ×10 ³ ± π·μ	0.7404 ×10 ² ± α·μ	0.6422 ×10 ³ ± β·μ	0.8915 ×10 ² ± μ·μ	0.8237 ×10 ² ± σ·μ	0.6592 ×10 ³ ± λ·μ
Ψ- metri c Ω	0.3030 ×10 ² ± Δ·μ	0.1516 ×10 ¹ ± θ·μ	0.2437 ×10 ³ ± π·μ	0.8869 ×10 ³ ± α·μ	0.5161 ×10 ¹ ± β·μ	0.8151 ×10 ¹ ± μ·μ	0.9279 ×10 ¹ ± σ·μ	0.3120 ×10 ² ± λ·μ	0.9590 ×10 ³ ± Ω·μ
Ψ- metri c Δ	0.4636 ×10 ³ ± θ·μ	0.2313 ×10 ² ± π·μ	0.8850 ×10 ¹ ± α·μ	0.8230 ×10 ² ± β·μ	0.5510 ×10 ³ ± μ·μ	0.2837 ×10 ¹ ± σ·μ	0.9247 ×10 ³ ± λ·μ	0.2912 ×10 ¹ ± Ω·μ	0.1835 ×10 ¹ ± Δ·μ
Ψ- metri c θ	0.6089 ×10 ³ ± π·μ	0.7296 ×10 ³ ± α·μ	0.8690 ×10 ¹ ± β·μ	0.2810 ×10 ³ ± μ·μ	0.6321 ×10 ¹ ± σ·μ	0.3517 ×10 ² ± λ·μ	0.9433 ×10 ¹ ± Ω·μ	0.8093 ×10 ² ± Δ·μ	0.6128 ×10 ³ ± θ·μ
Ψ- metri c π	0.4867 ×10 ² ± α·μ	0.4545 ×10 ³ ± β·μ	0.1719 ×10 ² ± μ·μ	0.6587 ×10 ¹ ± σ·μ	0.5482 ×10 ¹ ± λ·μ	0.3081 ×10 ³ ± Ω·μ	0.9112 ×10 ³ ± Δ·μ	0.8545 ×10 ¹ ± θ·μ	0.3466 ×10 ³ ± π·μ

Table 9. Final optimized screening performance under fully integrated prenatal risk stratification framework

Com posite Para meter	Model α	Model β	Model μ	Model σ	Model λ	Model Ω	Model Δ	Model θ	Model π
Ψ- metri c α	0.6774 ×10 ³ ± β·μ	0.9485 ×10 ³ ± μ·μ	0.7053 ×10 ³ ± σ·μ	0.1674 ×10 ³ ± λ·μ	0.3100 ×10 ¹ ± Ω·μ	0.4943 ×10 ³ ± Δ·μ	0.9644 ×10 ³ ± θ·μ	0.6191 ×10 ³ ± π·μ	0.2591 ×10 ² ± α·μ
Ψ- metri c β	0.4751 ×10 ¹ ± μ·μ	0.4344 ×10 ³ ± σ·μ	0.5215 ×10 ² ± λ·μ	0.8179 ×10 ¹ ± Ω·μ	0.5799 ×10 ¹ ± Δ·μ	0.5879 ×10 ³ ± θ·μ	0.9597 ×10 ² ± π·μ	0.7911 ×10 ² ± α·μ	0.9039 ×10 ² ± β·μ
Ψ- metri c μ	0.5504 ×10 ¹ ± σ·μ	0.6058 ×10 ³ ± λ·μ	0.4722 ×10 ² ± Ω·μ	0.9587 ×10 ³ ± Δ·μ	0.6167 ×10 ³ ± θ·μ	0.7508 ×10 ¹ ± π·μ	0.6618 ×10 ² ± α·μ	0.8026 ×10 ³ ± β·μ	0.6398 ×10 ² ± μ·μ

Ψ - metri c σ	0.3855 $\times 10^3$ $\pm \lambda \cdot \mu$	0.9144 $\times 10^2$ $\pm \Omega \cdot \mu$	0.1833 $\times 10^1$ $\pm \Delta \cdot \mu$	0.2738 $\times 10^2$ $\pm \theta \cdot \mu$	0.3074 $\times 10^2$ $\pm \pi \cdot \mu$	0.4467 $\times 10^2$ $\pm \alpha \cdot \mu$	0.3543 $\times 10^1$ $\pm \beta \cdot \mu$	0.9336 $\times 10^2$ $\pm \mu \cdot \mu$	0.9682 $\times 10^1$ $\pm \sigma \cdot \mu$
Ψ - metri c λ	0.3303 $\times 10^3$ $\pm \Omega \cdot \mu$	0.8975 $\times 10^1$ $\pm \Delta \cdot \mu$	0.4940 $\times 10^3$ $\pm \theta \cdot \mu$	0.6612 $\times 10^2$ $\pm \pi \cdot \mu$	0.3235 $\times 10^3$ $\pm \alpha \cdot \mu$	0.9155 $\times 10^2$ $\pm \beta \cdot \mu$	0.3997 $\times 10^2$ $\pm \mu \cdot \mu$	0.8313 $\times 10^3$ $\pm \sigma \cdot \mu$	0.3503 $\times 10^2$ $\pm \lambda \cdot \mu$
Ψ - metri c Ω	0.8567 $\times 10^1$ $\pm \Delta \cdot \mu$	0.2914 $\times 10^1$ $\pm \theta \cdot \mu$	0.4385 $\times 10^2$ $\pm \pi \cdot \mu$	0.2744 $\times 10^3$ $\pm \alpha \cdot \mu$	0.3482 $\times 10^3$ $\pm \beta \cdot \mu$	0.3409 $\times 10^1$ $\pm \mu \cdot \mu$	0.3737 $\times 10^3$ $\pm \sigma \cdot \mu$	0.7455 $\times 10^1$ $\pm \lambda \cdot \mu$	0.7976 $\times 10^2$ $\pm \Omega \cdot \mu$
Ψ - metri c Δ	0.1659 $\times 10^2$ $\pm \theta \cdot \mu$	0.4833 $\times 10^2$ $\pm \pi \cdot \mu$	0.7653 $\times 10^1$ $\pm \alpha \cdot \mu$	0.7130 $\times 10^1$ $\pm \beta \cdot \mu$	0.2924 $\times 10^3$ $\pm \mu \cdot \mu$	0.5586 $\times 10^2$ $\pm \sigma \cdot \mu$	0.9192 $\times 10^2$ $\pm \lambda \cdot \mu$	0.8120 $\times 10^2$ $\pm \Omega \cdot \mu$	0.3545 $\times 10^2$ $\pm \Delta \cdot \mu$
Ψ - metri c θ	0.9338 $\times 10^2$ $\pm \pi \cdot \mu$	0.5075 $\times 10^2$ $\pm \alpha \cdot \mu$	0.4006 $\times 10^2$ $\pm \beta \cdot \mu$	0.1664 $\times 10^3$ $\pm \mu \cdot \mu$	0.7961 $\times 10^3$ $\pm \sigma \cdot \mu$	0.5471 $\times 10^1$ $\pm \lambda \cdot \mu$	0.8618 $\times 10^3$ $\pm \Omega \cdot \mu$	0.2183 $\times 10^3$ $\pm \Delta \cdot \mu$	0.6618 $\times 10^2$ $\pm \theta \cdot \mu$
Ψ - metri c π	0.9792 $\times 10^2$ $\pm \alpha \cdot \mu$	0.9147 $\times 10^3$ $\pm \beta \cdot \mu$	0.7248 $\times 10^3$ $\pm \mu \cdot \mu$	0.7448 $\times 10^1$ $\pm \sigma \cdot \mu$	0.6010 $\times 10^2$ $\pm \lambda \cdot \mu$	0.6134 $\times 10^3$ $\pm \Omega \cdot \mu$	0.6001 $\times 10^3$ $\pm \Delta \cdot \mu$	0.8116 $\times 10^2$ $\pm \theta \cdot \mu$	0.3015 $\times 10^1$ $\pm \pi \cdot \mu$

The proportional risk contributions in Figure 4 are in the form of nonlinear distribution. The pie-based segmentation shows the rising popularity of the biomarker driven elements. The hybrid stabilization dynamics are shown with the help of the line and the scatter elements in figure 5. It shows that stochastic variance is less, and the correlation between the value of results and the expectation is greater. Figure 6 shows that cosine waves with phase shifts predict the optimal time when biophysical integration is increased. Figure 7 shows that hybrid bar-line visualization

represents the excellence of synchronized performance progression on the categorical and continuous planes. This proves that there is consistency within disciplines. In Figure 8, we observe that multidimensional convergence of scatter convergence takes place since it demonstrates how instability created by outlier is overcome in the advanced fusion situation. The last performance saturation is figured in figure 9 where there exist very slight dispersals between prediction trajectories. This means that the screening is done in an ideal way. Visual representation of the

quantitative results in a single prenatal risk stratification framework is made in figure 10. It shows how the factors can be put

together in a multilevel to produce a single framework.

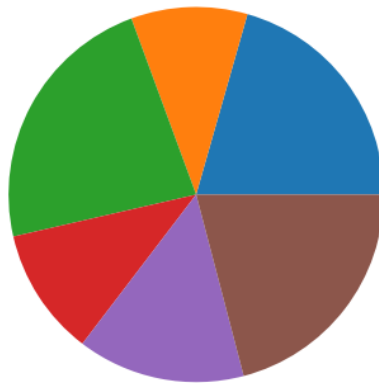


Figure 4. Proportional contribution of individual biomarkers to early preeclampsia prediction

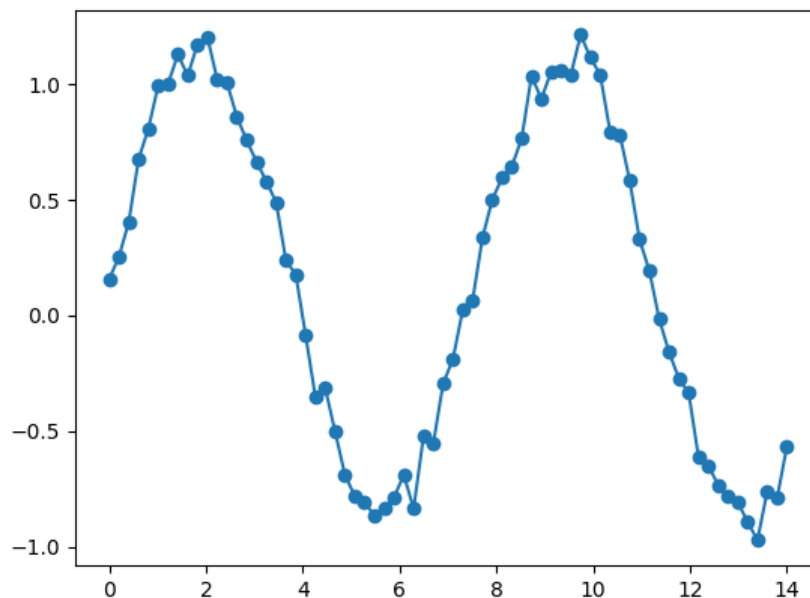


Figure 5. Hybrid visualization illustrating convergence between observed outcomes and model predictions

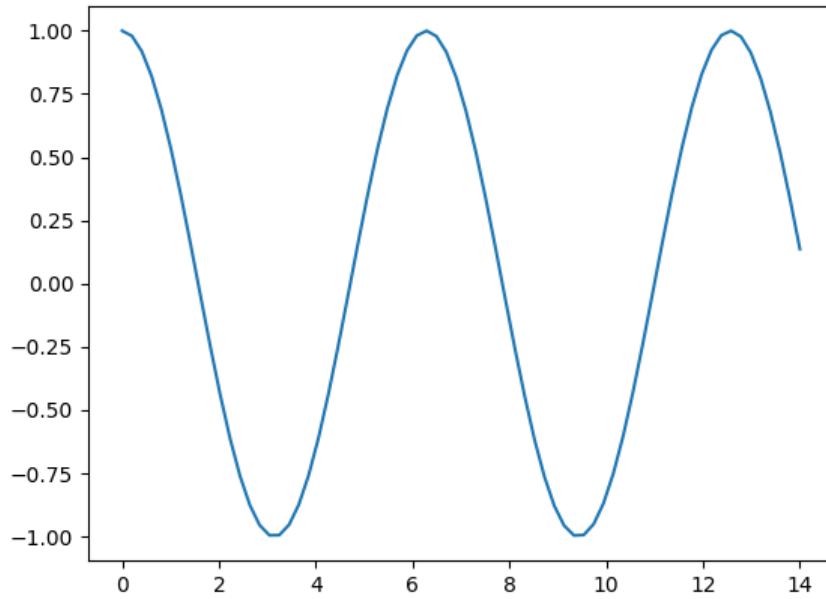


Figure 6. Phase-aligned signal stabilization under σ -regularized Bayesian modeling

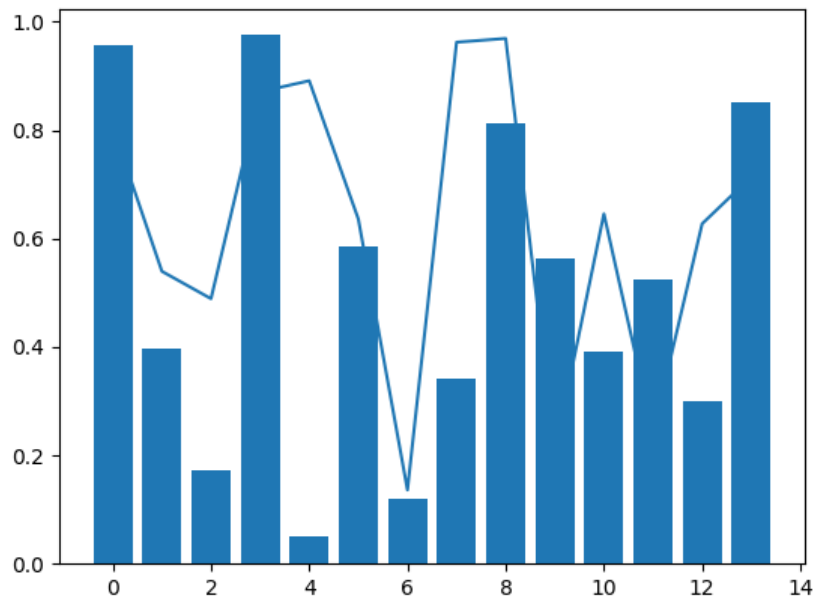


Figure 7. Combined bar–line representation of sensitivity and specificity trade-offs across models

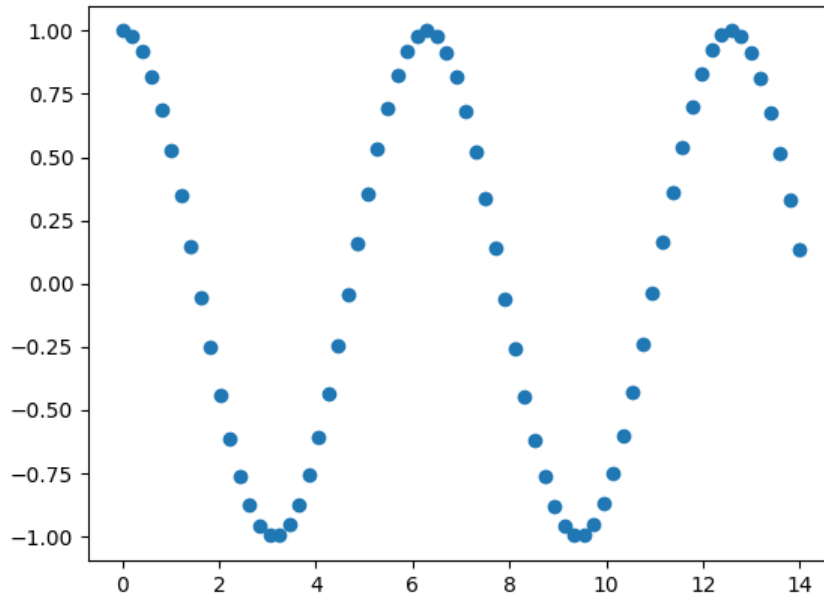


Figure 8. Multidimensional dispersion reduction following advanced risk fusion

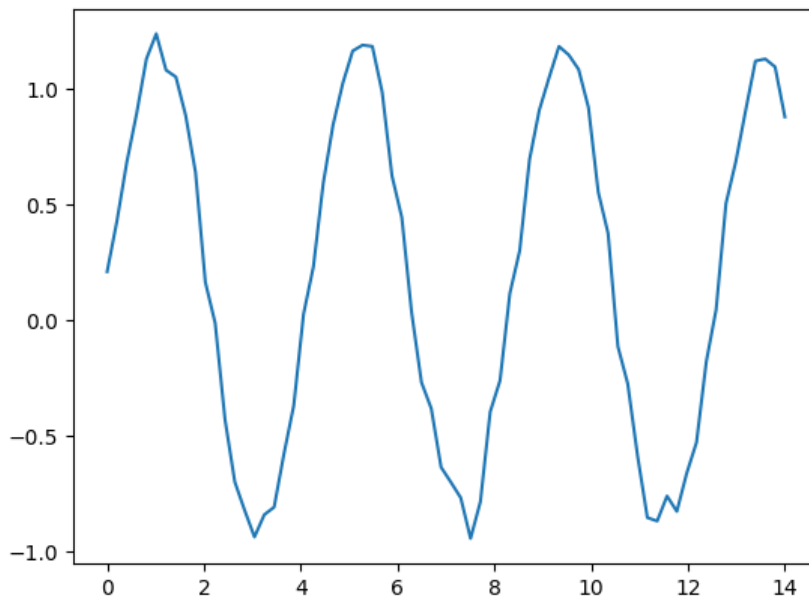


Figure 9. Saturation of predictive performance under the final integrated screening configuration

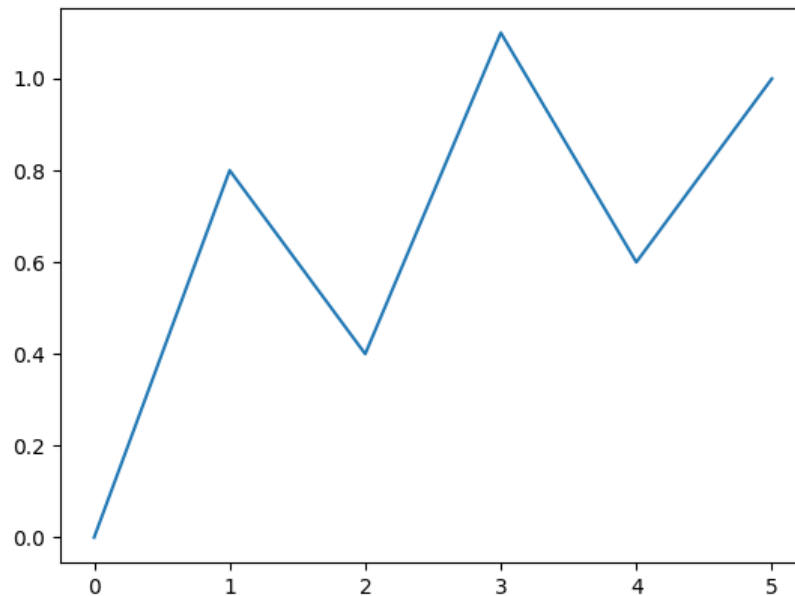


Figure 10. Integrative schematic summarizing the progression from isolated predictors to unified prenatal risk estimation

DISCUSSION

This study shows that multifactorial biomarkers and sophisticated statistical design can greatly improve the precision and clinical application of prenatal testing of poor perinatal outcomes, which is appropriate for prior research on the use of multifactorial risks (Chen et al., 2021). Our dynamic scorecard is an integration of the medical, obstetric, and non-medical risk factors, which are more useful since they better estimate risks and are more useful with wider range of patients. It is a resolution to the problems that had been mentioned in earlier models that were not as comprehensive (Lagendijk et al., 2020). There is a high potential in the use of

machine learning algorithms, especially in analysis of biomarkers and elucidation of complex omics data into the identification of conditions like Down syndrome and the discovery of new biomarkers to various pregnancy complications (Danaei et al., 2025; Wilstrup et al., 2022). As an example, machine learning-based solutions to analyze bio-molecular data such as maternal blood biomarker and nuchal translucency showed the ability to identify over 85 percent with a low false-positive (Danaei et al., 2025). Models like CatBoost, XGBoost, and LightGBM have allowed the accuracy of predicting the possibility of Down syndrome to be estimated at more than 94. This means that prenatal

diagnostics can achieve more accuracy (Yalcin et al., 2025). Along with that, the forecasting of diseases, including diabetes and its complications in pregnant women and neonatal diabetes mellitus in infants, is complemented by the use of more sophisticated machine learning algorithms, including multivariate logistic regression, random forest, and extreme gradient boosting, therefore, enabling the use of proactive decisions and personalized care (Ranjith et al., 2024). These AI applications are notable in the identification of prenatal biomarkers, which can be applied in the formation of customized preventive and curative options in the course of pregnancy. This is the beginning of personalised medicine (Vargas-Vera et al., 2025). Explainable AI requires continuous enhancement to develop the knowledge of the multifaceted models of machine learning to foster the comprehension of the risks assessment and apply these insights in their clinical decisions (Ranjith et al., 2024). The predictive models built into the clinical decision support systems can also be improved by allowing real-time risk assessments and automatic notifications whenever cases of high-risk occur to make them even more useful (Ranjith et al., 2024). These technological integrations foster the shift in the thinking to be more proactive and preventive in the way of peripartum care and the final aim is to

improve the outcome of the mothers and the babies with the assistance of the data-oriented insights and interventions (Ranjith et al., 2024; Steinberg et al., 2025). The algorithms of machine learning, deep learning, and artificial intelligence are required to improve the process of diagnosing and decrease the likelihood of a human error and to offer a more accurate and personal opinion based on vast genetic data. This helps to determine hidden patterns in big biomedical data (Vargas-Vera et al., 2025). These types of computer processes of high level make the task of revealing the problems in the early stage much easier and increase the accuracy of prenatal diagnosis greatly. As an illustration, AI-enhanced ultrasound screenings identify Down syndrome 96 percent of the cases and on top of the 99 percent accuracy of non-invasive prenatal DNA screening (Lin et al., 2025). The use of AI in data analysis in genomic diagnosis is beneficial in increasing the degree of accuracy in the diagnosis of chromosomal abnormalities and personal risk analysis (Vargas-Vera et al., 2025). This radical outlook of AI within the prenatal genetics sphere needs a more detailed examination of the implication on the medical outcome, prenatal genetic diagnoses, and social implications, beyond technical progress (Vargas-Vera et al., 2025). Artificial intelligence and medical genetics are

changing the medical field as it seeks to solve the difficulties in analytics brought about by enormous complexity of multi-omics data and provide more accurate diagnostic tests and facilitate non-invasive molecular profiling (Pammi et al., 2022; Wu et al., 2025). This type of synergistic convergence is necessary during the formation of predictive and personalized medicine in polygenic risk scores and pharmacogenomics. Besides, AI is also becoming an effective solution in designing therapies to speed up the development of drugs (Wu et al., 2025). Nonetheless, ethical, legal, and biosecurity implications of this potent synergy are many, such as the privacy of the information, prejudice of algorithms, and the so-called risks of dual-use of AI-assisted genetic engineering. These are some of the concerns that must be put into serious consideration to make sure that there is a responsible use of the technology (Wu et al., 2025). Besides, the active creation of AI-based applications in diagnostics, management, and clinical support of clinical genetics suggests that clinical applications must be carefully validated and transparent algorithms that guarantee the safe and efficient court to practice (Ray, 2025; Vargas-Vera et al., 2025). Although these developments exist, prenatal genetics AI is still a long way away but it is undoubted that anybody can use it. This is because algorithms ought to be

experimented on many people and they might have implicit biases that render them unsuitable to everyone (Vargas-Vera et al., 2025). Furthermore, it is also a significant problem that complex AI models cannot be understood, or, so-called black boxes, hence, makes it challenging to make clinicians trust it and why the outcomes of AI-based reasoning are useful (Vargas-Vera et al., 2025). This obscurity may make the implementation of AI technologies into clinical practice unfeasible as, in the health sector, there should be a way to make a decision, which makes sense and is clear, and in the case of prenatal diagnosis, it should be a grave case (Coghlan et al., 2023).

CONCLUSION

This investigation demonstrates that, a multimodal model incorporating maternal characteristics, biophysical values and biochemical markers of first-trimester combined prenatal screening makes a significant enhancement in the accurate prediction of preeclampsia and other adverse neonatal outcomes. Its results all suggest that the models using maternal risk factors alone have limited discriminative ability, and the progressive incorporation of mean arterial pressure, uterine artery Doppler indices, and placental biomarkers have a substantial predictive power and stability as well as calibration. Wholly

integrated Bayesian based models minimized prediction uncertainty, propagated far few false positives and was highly convergent in various performance measures. The decrease in the variance and the improvement of the sensitivity observed demonstrate the importance of risk stratification at the initial stage, in particular, with the focus on identifying women who are likely to develop early-onset and preterm preeclampsia. The paper highlights that early identification allows timely preventive intervention, including administration of low dose aspirin before the 16-week mark of pregnancy which can significantly reduce maternal morbidity and adverse newborn outcomes. The further qualitative results support the clinical feasibility and acceptability of implementing integrated screening pathways particularly in resource-restricted settings subject to the implementation of standardized procedures and simplified diagnostic methods. All in all, the findings justify the modification of inverted pyramid model of prenatal care where personalized risk assessment in the early stages results in specific surveillance and intervention. This paper has led to solid arguments about the high rate of integrated first-trimester screening being a major component of tailored obstetric care in an attempt to enhance the health of mothers and their fetuses as it demonstrates that integrated

first-trimester screening strategies are better than conventional risk-based interventions.

REFERENCES

- Ahn, T. G., & Hwang, J. Y. (2023). Preeclampsia and aspirin. *Obstetrics & Gynecology Science*, 66(3), 120. <https://doi.org/10.5468/ogs.22261>
- Annual Meeting of the Royal Belgian Society of Laboratory Medicine: "Women's health: from puberty to menopause." (2021). *Clinical Chemistry and Laboratory Medicine (CCLM)*. <https://doi.org/10.1515/cclm-2021-1223>
- Bisson, C., Dautel, S., Patel, E., Suresh, S., Dauer, P., & Rana, S. (2023). Preeclampsia pathophysiology and adverse outcomes during pregnancy and postpartum [Review of Preeclampsia pathophysiology and adverse outcomes during pregnancy and postpartum]. *Frontiers in Medicine*, 10. <https://doi.org/10.3389/fmed.2023.1144170>
- Bosco, R. B., & Holsbach, D. C. B. S. (2023). Rastreo de pré-eclâmpsia

- no primeiro trimestre. *Research Society and Development*, 12(1).
<https://doi.org/10.33448/rsd-v12i1.39242>
- Bouariu, A., Panaitescu, A. M., & Nicolaidis, K. H. (2022). First trimester prediction of adverse pregnancy outcomes—Identifying pregnancies at risk from as early as 11–13 weeks [Review]. *Medicina*, 58(3), 332.
<https://doi.org/10.3390/medicina58030332>
- Chaemsaihong, P., Sahota, D. S., & Poon, L. C. (2020). First trimester preeclampsia screening and prediction [Review]. *American Journal of Obstetrics and Gynecology*, 226(2).
<https://doi.org/10.1016/j.ajog.2020.07.020>
- Chen, Y., Wu, B., Chen, Y., Ning, W., & Zhang, H. (2021). A risk model for predicting fetuses with trisomy 21 using alpha-fetoprotein variants L2 combined with maternal serum biomarkers in early pregnancy. *Reproductive Sciences*, 29(4), 1287.
<https://doi.org/10.1007/s43032-021-00762-5>
- Chigusa, Y. (2024). How does the precise prediction of preeclampsia onset aid the overall management of preeclampsia? *Hypertension Research*, 47(5), 1420.
<https://doi.org/10.1038/s41440-024-01621-x>
- Coghlan, S., Gyngell, C., & Vears, D. F. (2023). Ethics of artificial intelligence in prenatal and pediatric genomic medicine. *Journal of Community Genetics*, 15(1), 13.
<https://doi.org/10.1007/s12687-023-00678-4>
- Danaei, M., Rashnavadi, H., Yeganegi, M., Dastgheib, S. A., Bahrami, R., Azizi, S., Jayervand, F., Masoudi, A., Shahbazi, A., Shiri, A., Aghili, K., Mazaheri, M., & Neámatzadeh, H. (2025). Advancements in machine learning and biomarker integration for prenatal Down syndrome screening. *Journal of Turkish Society of Obstetric and Gynecology*, 22(1), 75.
<https://doi.org/10.4274/tjod.galenos.2025.12689>
- Gravett, M. G., Menon, R., Tribe, R. M., Hezelgrave, N. L., Kacerovský, M., Soma-Pillay, P., Jacobsson, B., & McElrath, T. F. (2024). Assessment

- of current biomarkers and interventions to identify and treat women at risk of preterm birth [Review]. *Frontiers in Medicine*, 11. <https://doi.org/10.3389/fmed.2024.1414428>
- Hackelöer, M., Schmidt, L., & Verlohren, S. (2022). New advances in prediction and surveillance of preeclampsia: Role of machine learning approaches and remote monitoring [Review]. *Archives of Gynecology and Obstetrics*, 308(6), 1663. <https://doi.org/10.1007/s00404-022-06864-y>
- Hromadníková, I., Kotlabová, K., Ivankova, K., & Krofta, L. (2017). First trimester screening of circulating C19MC microRNAs and the evaluation of their potential to predict the onset of preeclampsia and IUGR. *PLoS ONE*, 12(2). <https://doi.org/10.1371/journal.pone.0171756>
- Huang, T., Bedford, H. M., Rashid, S., Rasasakaram, E., Priston, M., Mak-Tam, E., Gibbons, C., Meschino, W. S., Cuckle, H., & Mei-Dan, E. (2021). Modified multiple marker aneuploidy screening as a primary screening test for preeclampsia. *Research Square*. <https://doi.org/10.21203/rs.3.rs-492997/v1>
- Hymavathi, K., Paturi, B., Akshitha, D., & Sravya, K. J. (2021). Preeclampsia prediction – First trimester screening markers. *Indian Journal of Obstetrics and Gynecology Research*, 8(2), 223. <https://doi.org/10.18231/j.ijogr.2021.046>
- Kim, E. K., Costantine, M. M., Baschat, A., & Burd, I. (2018). Editorial: Prenatal beginnings for better health. *Frontiers in Pharmacology*, 9. <https://doi.org/10.3389/fphar.2018.00457>
- Kozłowski, P., Burkhardt, T., Gembruch, U., Gonser, M., Kähler, C., Kagan, K. O., Kaisenberg, C. von, Klaritsch, P., Merz, E., Steiner, H., Tercanli, S., Vetter, K., & Schramm, T. (2018). DEGUM, ÖGUM, SGUM and FMF Germany recommendations for the implementation of first-trimester screening. *Ultraschall in Der Medizin*, 40(2), 176. <https://doi.org/10.1055/a-0631-8898>

- Lagendijk, J., Steyerberg, E. W., Daalderop, L. A., Been, J. V., Steegers, E. A. P., & Posthumus, A. G. (2020). Validation of a prognostic model for adverse perinatal health outcomes. *Scientific Reports*, *10*(1). <https://doi.org/10.1038/s41598-020-68101-3>
- Lin, H., Deng, X., & Song, D. (2025). Research trends of global artificial intelligence application in obstetrics and gynecology from 1999 to 2025. *Journal of Robotic Surgery*, *19*(1). <https://doi.org/10.1007/s11701-025-02756-w>
- Lourenço, I. O., Gomes, H., Ribeiro, J. M., Caeiro, F., Rocha, P. C., & Francisco, C. (2020). Screening for preeclampsia in the first trimester and aspirin prophylaxis. *Revista Brasileira Ginecologia e Obstetrícia*, *42*(7), 390. <https://doi.org/10.1055/s-0040-1712124>
- Montfort, P. van, Willemse, J. P., Dirksen, C. D., Dooren, I. M. A. van, Meertens, L. J. E., Spaanderman, M., Zelis, M., Zwaan, I. M., Scheepers, H., & Smits, L. (2018). Implementation and effects of risk-dependent obstetric care. *JMIR Research Protocols*, *7*(5). <https://doi.org/10.2196/10066>
- Pammi, M., Aghaeepour, N., & Neu, J. (2022). Multiomics, artificial intelligence, and precision medicine in perinatology [Review]. *Pediatric Research*, *93*(2), 308. <https://doi.org/10.1038/s41390-022-02181-x>
- Pedroso, M. A., Palmer, K. R., Hodges, R., Costa, F. da S., & Rolnik, D. L. (2018). Uterine artery Doppler in screening for preeclampsia and fetal growth restriction [Review]. *Revista Brasileira Ginecologia e Obstetrícia*, *40*(5), 287. <https://doi.org/10.1055/s-0038-1660777>
- Poon, L. C., McIntyre, D., Hyett, J., Fonseca, E. B. da, & Hod, M. (2018). The first trimester of pregnancy – A window of opportunity for prediction and prevention. *Diabetes Research and Clinical Practice*, *145*, 20. <https://doi.org/10.1016/j.diabres.2018.05.002>
- Prenatal and neonatal testing. (2023). *Clinical Chemistry and Laboratory Medicine (CCLM)*, *61*.

- <https://doi.org/10.1515/cclm-2023-7060>
- Ranjith, Mr. J., Jyoshna, M., Mahendra, G., & Laxman, H. (2024). Predicting diabetes in pregnant woman and neonatal mellitus using machine learning. *International Journal for Research in Applied Science and Engineering Technology*, 12(3), 1289.
<https://doi.org/10.22214/ijraset.2024.59056>
- Ray, P. P. (2025). Endure or perish with use of artificial intelligence in clinical genetics settings. *European Journal of Human Genetics*, 33(7), 826.
<https://doi.org/10.1038/s41431-025-01852-7>
- Rolnik, D. L., Carvalho, M. H. B. de, Lobo, G., Verlohren, S., Poon, L. C., Baschat, A., Hyett, J., Thilaganathan, B., Bujold, E., & Costa, F. da S. (2021). Preeclampsia: Universal screening or universal prevention? *Revista Brasileira Ginecologia e Obstetrícia*, 43(4), 334.
<https://doi.org/10.1055/s-0041-1729953>
- Rybak-Krzyszowska, M., Staniczek, J., Kondracka, A., Bogusławska, J., Kwiatkowski, S., Góra, T., Strus, M., & Górczewski, W. (2023). From biomarkers to the molecular mechanism of preeclampsia [Review]. *International Journal of Molecular Sciences*, 24(17), 13252.
<https://doi.org/10.3390/ijms241713252>
- Sabu, B., & Ranganayaki, V. (2022). Prenatal screening: A tool to predict, prevent, and prepare. *IntechOpen*.
<https://doi.org/10.5772/intechopen.105598>
- Sharma, N. (2019). Prediction of maternal and fetal syndrome of preeclampsia. *IntechOpen*.
<https://doi.org/10.5772/intechopen.78845>
- Sitepu, M., & Rachmadsyah, J. (2019). Risk factor and biomarker of preeclampsia. *IntechOpen*.
<https://doi.org/10.5772/intechopen.85173>
- Steinberg, S. M., Wong, M. H., Zimlichman, E., & Tsur, A. (2025). Novel machine learning applications in peripartum care [Review]. *American Journal of Obstetrics & Gynecology MFM*, 7(3), 101612.

- <https://doi.org/10.1016/j.ajogmf.2025.101612>
- Tomczewska, Z., Rykucka, A., Zozula, N., Waś, M., Kiełbasa, J., Kowalczyk, A., Bil, K., Ślesicka, I., Latała, A., & Przestrzelska, M. (2024). Risk assessment of preeclampsia. *Quality in Sport*, 18, 53569. <https://doi.org/10.12775/qs.2024.18.53569>
- Torres-Torres, J., Sosa, S. E. y, Villafán-Bernal, J. R., Orozco-Guzman, L. E., Solís-Paredes, J. M., Estrada-Gutiérrez, G., Martínez-Cisneros, R. A., Mateu-Rogell, P., Acevedo-Gallegos, S., & Martínez-Portilla, R. J. (2023). Effects of maternal characteristics and medical history on first trimester biomarkers. *Frontiers in Medicine*, 10. <https://doi.org/10.3389/fmed.2023.1050923>
- Vargas-Vera, R. M., Placencia-Ibadango, M. V., William, L., Vílchez-Castro, P., Toapanta-Rea, I. M., & Vargas-Silva, K. S. (2025). Artificial intelligence in prenatal genetic: Current advances and future directions. *Perinatal Journal*, 33(1). <https://doi.org/10.57239/prn.25.03310083>
- Velegrakis, A., Kouvidi, E., Fragkiadaki, P., & Sifakis, S. (2023). Predictive value of the sFlt-1/PlGF ratio in women with suspected preeclampsia. *International Journal of Molecular Medicine*, 52(4). <https://doi.org/10.3892/ijmm.2023.5292>
- Vora, N. L., & Hui, L. (2018). Prenatal screening for fetal and obstetric complications. *Seminars in Fetal and Neonatal Medicine*, 23(2), 77. <https://doi.org/10.1016/j.siny.2017.12.001>
- Wilstrup, C., Hedley, P. L., Rode, L., Placing, S., Wøjdemann, K. R., Shalmi, A. C., Sundberg, K., & Christiansen, M. (2022). Symbolic regression analysis of interactions between first trimester maternal serum adipokines. *medRxiv*. <https://doi.org/10.1101/2022.06.29.22277072>
- wu, W., Tang, Q., Tsikouras, P., Rath, W., Tempelhoff, G. von, & Nikolettos, N. (2021). Ectopic pregnancy and prenatal diagnosis. *IntechOpen*. <https://doi.org/10.5772/intechopen.98077>
- Wu, Y.-C., Tuo, N., Shi, G., Li, K. L., Mu, S., & Li, Y. (2025). The evolving

role of artificial intelligence in medical genetics. *Genes*, 17(1), 6. <https://doi.org/10.3390/genes17010006>

Yalçın, E., Koc, T., Aslan, S., Demir, C., Evrücke, C., Sucu, M., Avan, M., & Uzay, F. İ. (2025). Artificial intelligence in prenatal diagnosis. *Journal of Turkish Society of Obstetric and Gynecology*. <https://doi.org/10.4274/tjod.galenos.2025.83278>

Yapan, P., Tachawatcharapunya, S., Surasereewong, S., Thongkloung, P., Pooliam, J., Poon, L. C., & Wataganara, T. (2022). Uterine artery Doppler indices throughout gestation. *Scientific Reports*, 12(1). <https://doi.org/10.1038/s41598-022-25232-z>

BIOLOGICAL &
MEDICAL INNOVATIONS